



# Tea waste–derived charcoal as an efficient adsorbent for the removal of rhodamine B

Kanchan Bala<sup>1</sup> · Deepika Sharma<sup>2</sup> · Naveen Kumar<sup>3</sup> · Neeraj Gupta<sup>4</sup> · Vaseem Raja<sup>5</sup>

Received: 1 May 2023 / Revised: 10 August 2023 / Accepted: 27 August 2023  
© The Author(s), under exclusive licence to Springer-Verlag GmbH Germany, part of Springer Nature 2023

## Abstract

The current investigation demonstrates the efficacy of activated carbon derived from tea waste (ACTW) as a potent adsorbent for the elimination of rhodamine B (Rh-B), a cationic dye, from water. Several factors, including initial Rh-B concentration, solution pH, temperature, and contact time, were scrutinized to evaluate their impact on the adsorption process. Furthermore, attempts were made to establish a correlation between the isothermal data obtained through the application of the Langmuir, Freundlich, and Temkin equations. Kinetic modeling using pseudo-first-order and pseudo-second-order rate parameters was utilized to scrutinize the rate of the adsorption process. The data obtained were found to conform to the pseudo-second-order kinetic model. With the increase in the ACTW (adsorbate) dosage from 0.2 g to 1.8 g, the removal of Rh-B dye escalated from 76 to 97.8%. In contrast, the adsorption capacity decreased from 10.1 to 2.2 mg/g. Fourier-transform infrared spectra of ACTW illustrated humps located at 2927 cm<sup>-1</sup> and 2480 cm<sup>-1</sup>, which correspond to alkane and alkene groups (C–H stretching of CH<sub>2</sub> groups). Microstructural analysis of ACTW revealed porous granules with shattered surfaces. Thermodynamic parameters indicated that the adsorption process was spontaneous ( $\Delta G^\circ = \text{negative}$ ) and endothermic ( $\Delta H^\circ = \text{positive}$ ). The findings suggest that ACTW is an effective and potential adsorbent for removing Rh-B dye from aqueous solutions. Furthermore, the results of the study indicate that tea waste is a cost-effective and efficient adsorbent for removing cationic dyes from aqueous solutions.

**Keywords** Activated charcoal · Tea waste · Rh-B dye · Dye removal

## 1 Introduction

In the twenty-first century, the contamination of natural water sources due to the discharge of wastewater from various chemical industries and factories is a worldwide issue [1, 2]. Wastewater contains toxic pollutants such as heavy metals, dyes, pesticides, and industrial and pharmaceutical

waste products. These pollutants may not be involved in direct toxicity but generates hazardous byproduct through hydrolysis, chemical reactions, and oxidation. This may enhance chemical oxygen demand and biological oxygen demand that jeopardize the environment, microorganism, plants, animals, and aquatic and human life [3–5]. Approximately 15% of dyes get discharged into the environment or the running water after use [6]. The industrial and organic dyes are intractable, thermostable, rebellious, non-biodegradable, and stable oxidizing agents [7]. Rh-B dye is a widely used coloring in textiles and food products, manufacturing of paper, and leather dyeing [8]. This dye belongs to xanthine family and used in biological, optical, and analytical sciences. The hazardous Rh-B dye can create many problems including dysfunction of liver, kidney, brain, central nervous system, reproductive system, skin respiratory inflammation, and hemolysis [9]. For the environmental remediation, the development of the cost-effective and reliable approach to handle or remove the toxic dyes is a burning topic nowadays. The conventional dye removal methodologies (chemical, physical, biological) reported in

✉ Naveen Kumar  
naveensethi99@gmail.com

<sup>1</sup> Department of Chemistry, Government Mohindra College, Patiala 147001, India

<sup>2</sup> Department of Chemistry, IEC University, Baddi, Solan, Himachal Pradesh 174103, India

<sup>3</sup> Department of Physics, Chandigarh University, Gharuan, Punjab 140413, India

<sup>4</sup> Department of Chemistry and Chemical Science, Central University of Himachal Pradesh, Dharamshala, Kangra (H.P) 176213, India

<sup>5</sup> University Center for Research and Development, Gharuan, Punjab 140413, India

literature are sedimentation, ultrafiltration, adsorption, ion exchange, chemical oxidation, photocatalytic, and reverse osmosis [10–12]. Therefore, we used the adsorption method for the removal of contaminants from the aqueous solution [13]. Adsorption method is good enough due to its unique properties including ease of separation, stability, reusability, and mild solvent use [14]. Hence, an excessive consideration has been oriented towards using various adsorbents like graphene, nanocomposites, and carbon-based materials. Carbon-based materials are more preferable adsorbents used to remove Rh-B dye due to their enormous properties including high surface area, porosity, easy synthesis, high reactivity, and tuneable surface functional groups [15].

Carbon materials can be easily synthesized from waste residues, biomasses, and agricultural wastes including bagasse, wood products, coconut shell, peanut hull, paddy straws, and tea dust leaves. Moosavi et al. have used the activated carbon from coconut shell [16] as an adsorbent to remove the methylene blue dye from wastewater. Activated carbon is a highly effective adsorbent that can capture a wide range of organic substances through weak intermolecular forces, such as dispersion forces. These interactions can be further strengthened by  $\pi$ - $\pi$  interactions in the case of aromatic adsorbates or by electrostatic interactions between surface oxide groups and ionic adsorbates. The degree of adsorption is directly linked to the size of the adsorbate molecule, assuming that the size of the adsorbate does not surpass the dimensions of the pore system, which can result in size exclusion effects. Mitra and Mukharjee have reported the removal efficiency (85.25%) by using activated carbon as an adsorbent from spent tea leaves at 30°C temperature and it was further increased to 90.2% at the temperature 80–100°C [17]. Qui et al. reported the biochar derived from waste can be used for water remediation such as heavy metal detection and they also discussed about adsorption mechanism [18]. Biochar can be used effectively for adsorption and degradation of organic dyes, and removal of phenols and antibiotic from wastewater [19]. Another carbon-based structures such as ordered mesoporous carbon and graphitic carbon nitride have also been used to investigate as an adsorbate for photocatalytic activities [20, 21]. Ahmaruz-zaman and Gaytri examined activated tea waste as an adsorbent for removal of p-Nitrophenol from aqueous systems [22]. Olayinka et al. investigated tea waste, coconut shell, and coconut husk for removal of heavy metals such as Cr, Zn, and Ni [23]. Thapak et al. used activated tea waste to detect Cu, and Cr from synthetic wastewater [24].

Owing to aforementioned discussion of activated tea waste and their potential for heavy metal removal and dye degradation, in the present study, we are reporting synthesis of a very low cost “activated carbon from waste cooked tea” as an adsorbent for the removal of Rh-B dye from aqueous solution.

## 2 Experimental

### 2.1 Materials

Analytical grade hydrochloric acid (HCl), potassium manganate ( $\text{KMnO}_4$ ), sodiumhydroxide (NaOH), hydrogenperoxide ( $\text{H}_2\text{O}_2$ ), sulfuric acid ( $\text{H}_2\text{SO}_4$ ), and Rh-B were purchased from Merck (India) and used further without any modification or treatment.

### 2.2 Preparation of charcoal (adsorbent)

The source of the cooked tea waste material used in this experiment was the hostel mess of Baba Farid Group of Institution in Bathinda, Punjab, India. The tea waste was meticulously washed with distilled water to eliminate any colored soluble compounds. Following the washing process, the tea waste was dried in an oven at a temperature of 80 °C. Afterwards, the material was placed in a silica crucible and subjected to annealing inside a muffle furnace at a temperature of 500 °C for 30 min in an atmosphere of nitrogen to convert the tea waste into charcoal. Once the process was completed, the charcoal was allowed to cool for 4 h.

### 2.3 Activation of charcoal

The charcoal was activated through a rigorous oxidation process utilizing the modified Hummer’s method. The charcoal was placed in an Erlenmeyer flask and 100 mL of highly concentrated sulfuric acid was added while stirring continuously. The stirring process was continued for 30 min, and then potassium acetate was introduced to the solution. The mixture was then allowed to sit for 24 h. The activated sample was meticulously washed with a solution of hydrochloric acid (0.1 M) and distilled water to bring the pH to a neutral level. The filtered product was then dried in a hot oven at 60 °C overnight and subsequently crushed into a fine powder and leveled to form activated carbon derived from tea waste (ACTW).

### 2.4 Characterization of ACTW

The physicochemical properties of as-synthesized charcoal and ACTW were analyzed using Fourier transform infrared spectroscopy by Perkin Elmer, scanning electron microscopy (SEM) by Hitachi, and UV–visible spectrophotometer by Perkin Elmer (LAMBDA 365+). Brunauer–Emmett–Teller surface area analyzer was used to evaluate specific surface area and pore volume.

### 2.5 Preparation of dye solution

Rh-B dye ( $\text{C}_{28}\text{H}_{31}\text{N}_2\text{O}_3\text{Cl}$ ) having IUPAC name [9-(2-carboxyphenyl)-6-diethylamino-3-xanthenylidene]-

diethylammonium chloride is basic red dye of the xanthene class. Stock solution of dye was prepared by dissolving 0.5 g of dye in 1000 mL (500 mg/L) of distilled water. Different amounts of solution of desired concentration solution were prepared by dilutions of the stock solution.

A batch adsorption experiment for removal of Rh-B dye onto ACTW has been carried out as a function of adsorbent dose, initial dye concentration, contact time, pH, and temperature. Adsorption was achieved by adding a known amount of each adsorbent of a specific sieve size at room temperature at constant speed on mechanical shaker into the dye solution (100 mL) of known concentration and pH, and the conical flasks were agitated properly. Once the equilibrium was established, 5.0 mL of dye solution has been withdrawn at pre-determined time intervals and the absorbance was determined using spectrophotometer ( $\lambda_{\text{max}} = 554 \text{ nm}$ ). During adsorption, equilibrium has been established between adsorbed dye on active sites of adsorbent and unadsorbed dye in the solution.

The percentage of dye adsorbed and adsorption capacity at equilibrium was calculated by the formulae given below:

$$\text{Percentage adsorption (\%)} = \frac{(C_0 - C_e)}{C_0} \times 100 \quad (1)$$

$$\text{Adsorption capacity (q}_e\text{)} = \frac{(C_0 - C_e)}{W} \times V \quad (2)$$

where  $C_0$  and  $C_e$  represent the initial and final equilibrium concentrations (mg/L), and  $V$  is the volume of solution and  $W$  is the weight of adsorbent dose.

## 3 Results and discussion

### 3.1 Fourier transfer infrared spectroscopy analysis:

The functional groups attached to the organic and inorganic specimen can be detected using Fourier transfer infrared (FTIR) spectroscopy technique. The vibrating molecules of the attached groups lead to distinctive energies and depict kink in the FTIR spectra when recorded within 400 to 4000  $\text{cm}^{-1}$  at room temperature. Figure 1 illustrates FTIR spectrum of as-synthesized charcoal and ACTW. Figure 1 clearly indicates the differences in the spectral humps in as-synthesized charcoal and ACTW. The characteristic peaks of ACTW are observed at 2927  $\text{cm}^{-1}$ , 2480  $\text{cm}^{-1}$ , 1700  $\text{cm}^{-1}$ , 1520  $\text{cm}^{-1}$ , 1461  $\text{cm}^{-1}$ , 1314  $\text{cm}^{-1}$ , 1124  $\text{cm}^{-1}$ , 1013  $\text{cm}^{-1}$ , and 854  $\text{cm}^{-1}$ . The humps located at 2927  $\text{cm}^{-1}$  and 2480  $\text{cm}^{-1}$  corresponds to alkane and alkene groups (C–H stretching of  $\text{CH}_2$  groups) [25]. The kinks positioned at 1700  $\text{cm}^{-1}$  is attributed to  $\text{C}=\text{O}$  stretching vibrations

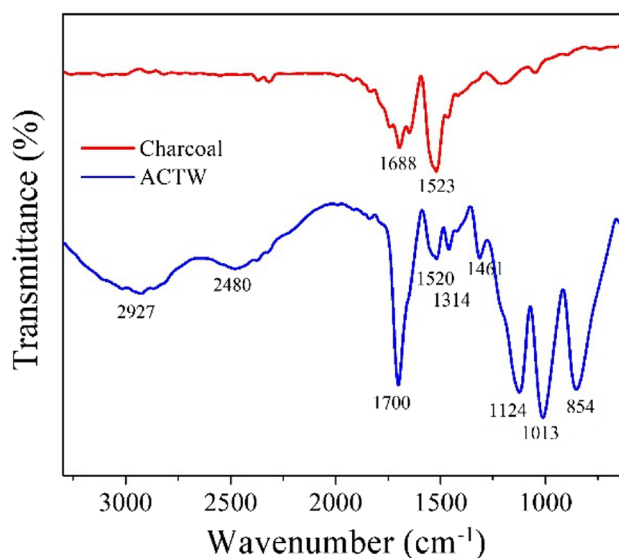
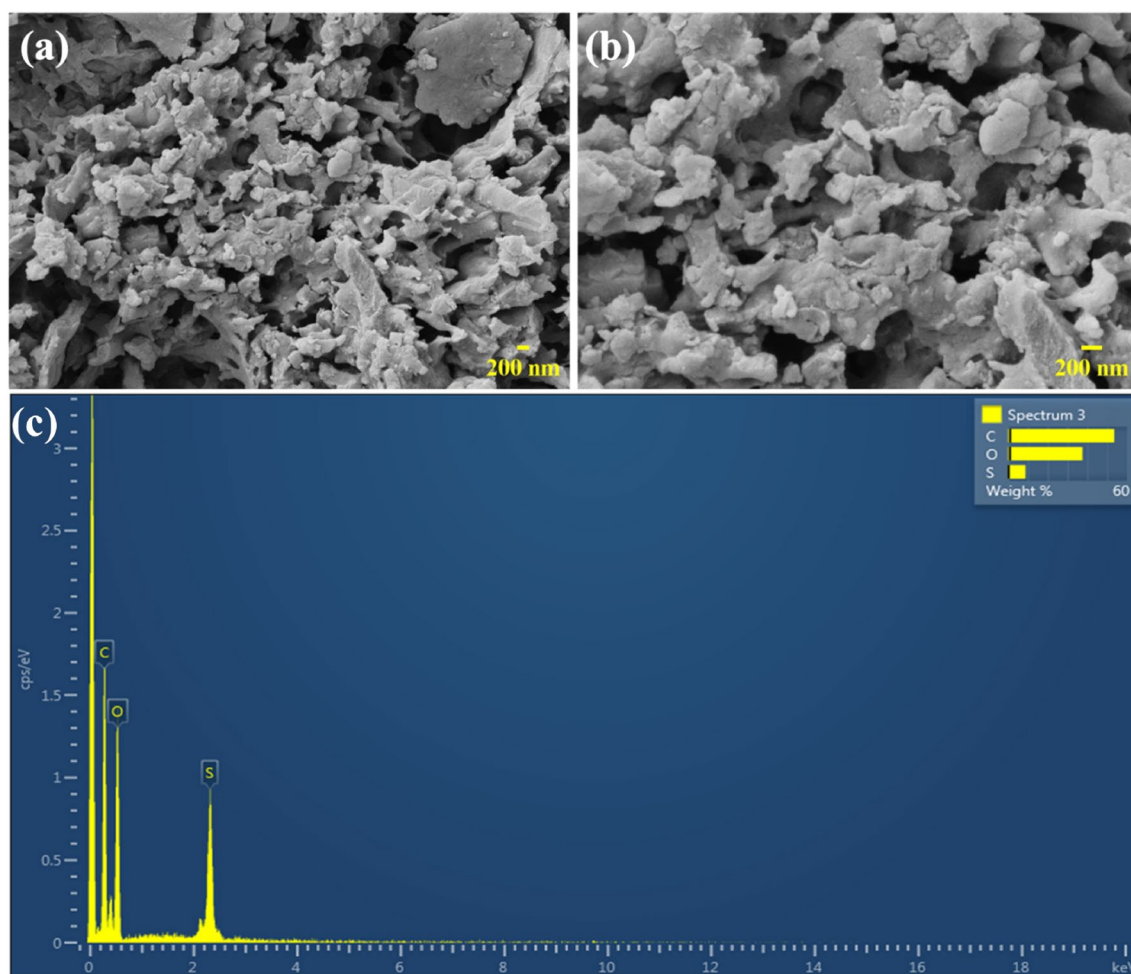


Fig. 1 FTIR spectra of charcoal and ATCW

[26]. The weak absorption bands appeared at 1124  $\text{cm}^{-1}$  and 1013  $\text{cm}^{-1}$  are mainly due to existence of  $\text{C}=\text{N}$  and  $\text{C}-\text{O}$  stretching modes belonging to polysaccharides like substances. The bend at 854  $\text{cm}^{-1}$  could be assigned to C–S linkage in the compound [27]. The kinks for charcoal are observed at 1688  $\text{cm}^{-1}$  and 1523  $\text{cm}^{-1}$  respectively which belongs to  $\text{C}=\text{C}$  stretching vibration and thereby confirms the formation of charcoal [28]. The relative existence of new umps in the ACTW supports the activation of charcoal after treatment.

### 3.2 Microstructural analysis

Surface morphology and granular microstructure of charcoal and ACTW was analyzed using SEM at room temperature. Microimages of derived charcoal and ACTW are illustrated in Fig. 2a and b. SEM micrograph displayed the external surface of the ACTW having crevices and various large-sized holes. It was concluded from the SEM images that the synthesized ACTW is highly porous in nature with the ruptured surface [29]. So, there are plenty of surfaces available for the adsorption of the dye. The elemental compositions present in the ACTW sample were analyzed using energy-dispersive spectroscopy (EDS). Figure 2c shows the EDS line spectrum of ACTW. Line profile spectrum depicts the existence of carbon (52.6 wt%), oxygen (37.5 wt%), and little amount of sulfur (8.8 wt%) in the sample. The specific surface area and pore volume of charcoal is 2.55  $\text{m}^2/\text{g}$  and 2.95  $\text{cc}/\text{g}$ , respectively, and for ACTW is 4.89  $\text{m}^2/\text{g}$  and 4.13  $\text{cc}/\text{g}$ , respectively. FTIR spectral studies also support the presence of sulfur which may be occurred due to utilization of  $\text{H}_2\text{SO}_4$  during synthesis or activating the charcoal.



**Fig. 2** a SEM micrographs of a charcoal, b ACTW, and c EDS spectra of ACTW

### 3.3 Batch adsorption studies

#### 3.3.1 Effect of adsorbent dose

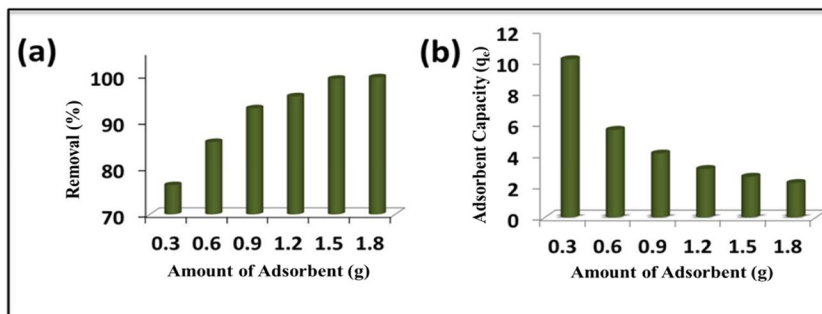
The quantity of adsorbent dose is the predominant parameter in adsorption study as it determines the capacity of adsorbent to remove the dye at a specific concentration. In this experiment, we varied the amount of ACTW from 0.2 g to 1.8 g (initial dye concentration = 40 mg/L, contact time = 50 min). It has been observed that percentage of dye removed increases from 76.0 to 97.8% and adsorption capacity decreases from 10.1 to 2.2 mg/g. It is attributed that by increasing the amount of adsorbent dose, the adsorptive surface area increases, due to which the number of available sites increases and results in increase in percentage removal of dye [30–32]. The 97.8% of dye removal is observed with 1.5 g of ACTW, but with more increase in adsorbent dose (1.8 g), there is a little effect on the removal percentages. The adsorption capacity ( $q_e$ ) decreases because number of adsorbate molecules remains constant, the remaining dye

molecules in the solution do not adsorb on the adsorbent. The effects of adsorbent dosage on the percentage removal and adsorption capacity of Rh-B dye are represented in Fig. 3a and b respectively. ACTW is found to porous and with an extensive high surface area. This enhanced surface area provides numerous active sites for the Rh-B dye molecules to interact with. Rh-B dye is a planar molecule containing conjugated electron systems. These  $\pi$ -electron clouds can interact with the  $\pi$ -electron systems present on the surface of activated charcoal. The resulting  $\pi$ - $\pi$  stacking interactions further contribute to the adsorption process.

#### 3.3.2 Effect of the contact time on adsorption

The impact of contact time on the adsorption of rhodamine B (Rh-B) dye onto ACTW was investigated by stirring a dye solution with varying concentrations together with the adsorbent at a constant speed and temperature. It was observed that the initial rate of adsorption was rapid due to the abundance of available adsorption sites, while as the

**Fig. 3** Initial dye concentration = 40 mgL<sup>-1</sup>, contact time = 50 min. **a** Effect of adsorbent dose on percentage removal of dye. **b** Effect of adsorbent dose on adsorption capacity of dye



contact time increased, the rate of adsorption decreased due to a reduction in active sites. The highest percentage of dye removal was achieved after 50 min of contact time. The adsorption mechanism involves the migration of dye from the bulk solution, diffusion through the boundary layer, and intra-particle diffusion into the interior pores of the adsorbent. This instantaneous adsorption phenomenon has the advantage of reducing contact time and equipment size, thereby minimizing the operational cost of the process.

### 3.3.3 Effect of initial adsorbate concentration

The relationship between the initial dye concentration and the adsorbent surface is of great significance. Figure 4a and b demonstrate the adsorption results of various initial dye concentrations (20, 40, 60, 80, and 100 mg/L) with 1.5 g of adsorbent at different time intervals. The data reveals that as the initial dye concentration increases, the percentage of dye removal decreases, indicating a saturation of the adsorbent surface's adsorption sites. Conversely, a higher initial concentration of the dye leads to an increase in the adsorption capacity, owing to the powerful force of mass transfer in high dye concentrations. At lower concentrations, the ratio of initial number of dye molecules to available surface is limited, while at higher concentrations the ratio of number of dye molecules to available surface becomes substantial.

### 3.3.4 Effect of pH

The pH of a solution is a crucial factor in determining the adsorption capacity of an adsorbent during wastewater treatment or dye removal. This is because changes in pH can alter the surface properties of the adsorbent, thereby affecting its adsorption efficiency. In order to investigate the impact of pH on the adsorption capacity of ACTW, a 40 mg/L solution of cationic Rh-B dye was stirred with 1.5 g of ACTW at room temperature under varying pH conditions (2.0, 4.0, 6.0, and 8.0). The results showed that the adsorption capacity of ACTW for Rh-B was highest at a low pH of 2.0, as illustrated in Fig. 5. This can be attributed to the polarization of the adsorbent surface under acidic conditions, which

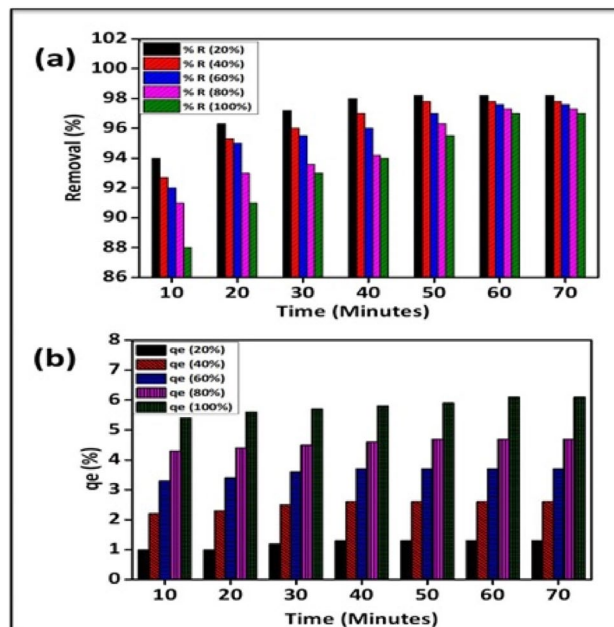


**Fig. 4 a** Effect of initial dye concentration and contact time on percentage removal (R%) of Rh-B dye. Initial dye concentration = 40 mg/L, contact time = 50 min, dose = 1.5 g. **b** Effect of initial dye concentration and contact time on adsorption capacity of dye. Initial dye concentration = 40 mg/L, contact time = 50 min, dose = 1.5 g

facilitates the adsorption of the dye molecules on the surface of the adsorbent.

### 3.3.5 Effect of temperature

The temperature is a key factor affecting the physico-chemical adsorption process, as it influences the adsorbent capacity. In this study, the effect of temperature on the removal of dye was investigated at 305 K, 311 K, and 317 K as shown in Fig. 6. The results demonstrated that the percentage of dye removal increased with rising temperature, indicating that the adsorption process is endothermic. This temperature dependence can be attributed to the enhanced mobility of the dye molecules at higher temperatures, leading to increased access to active

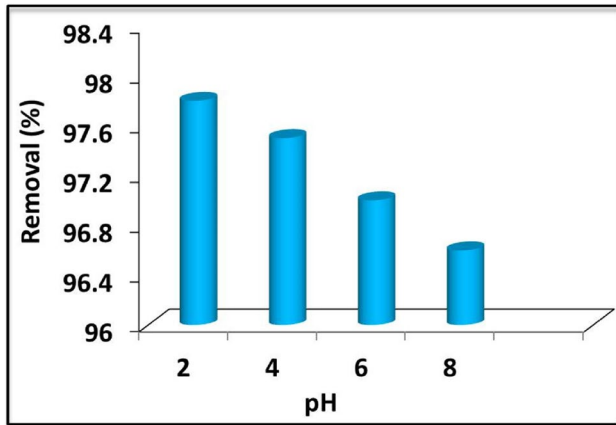


**Fig. 5** Effect of pH on percentage removal of Rh-B dye (initial dye concentration = 40 mg/L, contact time = 50 min)

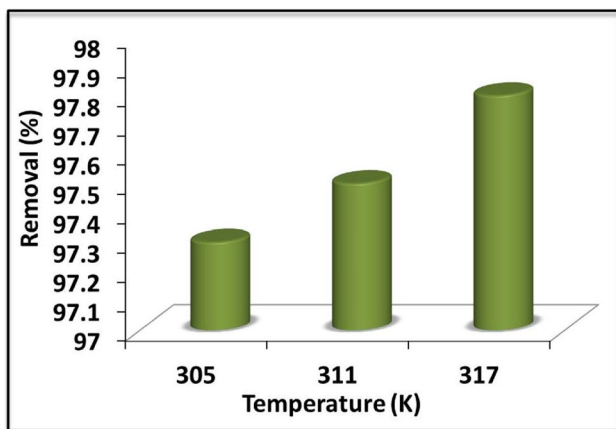


**Fig. 6** Effect of temperature on percentage removal of Rh-B dye (initial dye concentration = 40 mg/L, contact time = 50 min)

adsorption sites. This suggests that temperature can be used as a parameter to regulate the adsorption capacity of the adsorbent.

### 3.3.6 Kinetic models

Equilibrium adsorption isotherm models are essential requirements for the design of adsorption systems and the interaction between adsorbent and adsorbent. Models used to analyze equilibrium adsorption data include the Langmuir, Freundlich, and Temkin models.

### 3.3.7 Langmuir model

The Langmuir isotherm is a widely used model for describing the nonlinear equilibrium between an adsorbate and

its concentration in solution at constant temperature. This model assumes that adsorption occurs on a surface with a homogeneous structure and that a monolayer of adsorbate molecules is formed. It further assumes that all adsorption sites have the same energy and that the adsorption process is reversible. The Langmuir isotherm is a simple model that allows for the calculation of the maximum adsorption capacity of an adsorbent and the affinity of the adsorbate for the adsorbent. The linear equation for Langmuir relationship can be represented as [33]:

$$\frac{C_e}{q_e} = \frac{C_e}{q_{max}} + \frac{1}{q_{max}b_L} \quad (3)$$

$q_e$  is the amount of adsorbed analyte per unit mass of the adsorbent.

$q_{max}$  is the maximum amount of adsorption in the adsorbent monolayer in mg/g.

$C_e$  is the equilibrium concentration of analyte in solution in mg/L.

$b_L$  is langmuir equation constant.

$q_{max}$  and  $b_L$  are the Langmuir constants related to the maximum adsorption capacity (mg/g) and energy of adsorption (L/mg) is illustrated in Fig. 7. The essential characteristics of Langmuir isotherm can be expressed by a dimensionless constant called equilibrium parameter  $R_L$ , which is defined by equation:

$$R_L = \frac{1}{1 + b_L C_o} \quad (4)$$

The value of  $R_L$  indicated the type of Langmuir isotherm as tabulated in Table 1.

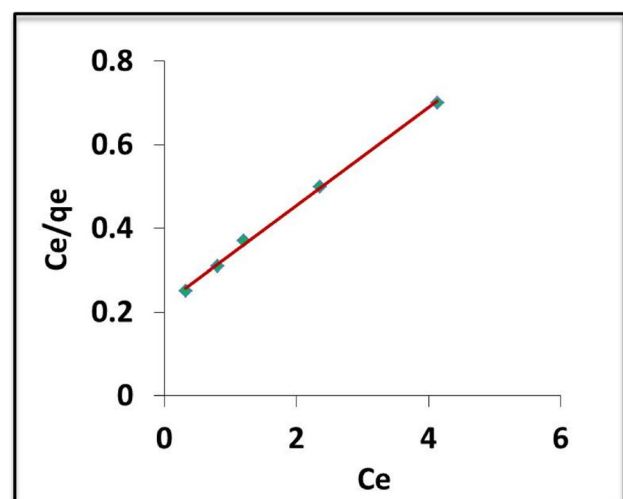


**Fig. 7** Langmuir adsorption isotherm for Rh-B adsorption at 305 K

The value of  $R_L$  was found to be 0.045, 0.032, and 0.021 for 40 mg/L concentration of Rh-B dye at 305 K, 311 K, and 317 K, respectively, which indicates the favorable adsorption.

### 3.3.8 Freundlich model

The Freundlich adsorption isotherm is an experiential model that characterizes adsorption on a heterogeneous surface and accounts for the concept of multilayer adsorption. The model suggests that there exist numerous adsorption sites on the surface, each having distinct free energy values. As per this theory, the surface never achieves complete saturation, even with a significant increase in solute concentration, since the presence of high free energy sites on the surface ensures adsorption continues to occur. The Freundlich isotherm can be mathematically represented by the following equation:

$$\log q_e = \log K_f + \frac{1}{n} \log C_e \tag{5}$$

where  $K_f$  is Freundlich constant that is related to the adsorption capacity,  $n$  is a constant related to the heterogeneity of the surface and describes the type of the Freundlich isotherm, and its value usually varies in the range of 0–1. The closer value of  $n$  to 1 means the more homogeneous surface. The type of relationship is given in Table 2. The Freundlich isotherm shows that a higher concentration of initial analyte would lead to a higher adsorption rate of adsorbent. It is evident from Freundlich adsorption isotherm as shown in Fig. 8 that the data fit well with having regression coefficient  $R^2=0.97$ . The values of  $K_f$  and  $1/n$  have been calculated from intercept and slope of this straight line are given in Table 3.

### 3.3.9 Temkin model

This model was given by Temkin and Pyzhevand; the linear form of Temkin isotherm model is given by the following equation:

$$q_e = B \ln K_T + B \ln C_e \tag{6}$$

where  $K_T$  and  $B$  are the constants related to adsorption capacity and intensity of adsorption, respectively. A linear plot between  $q_e$  versus  $\ln C_e$  shows that adsorption follows Temkin isotherm is illustrated in Fig. 9. The values of  $K_T$  and  $B$  have been evaluated from slope and intercept of the plot.

**Table 1** Correlation of  $R_L$  with the Langmuir isotherm

Isotherm situation	$R_L$
Undesirable	$R_L > 1$
Linear	$R_L = 1$
Desired	$0 < R_L < 1$
Reversible	$R_L = 0$

**Table 2** Correlation  $n$  with the Freundlich isotherm

Isotherm situation	$n$
Undesirable	$n > 1$
Linear	$n = 1$
Desired	$n < 1$

### 3.4 Kinetic studies

Many kinetic models have been applied to study the controlling mechanism of dye adsorption from aqueous solution. In order to investigate the mechanism of adsorption of Rh-B dye onto AWTC, the pseudo-first-order, pseudo-second-order, and intra particle diffusion kinetic models were considered:

#### 3.4.1 Pseudo-first-order

The integrated linear form of first order rate equation is as follows:

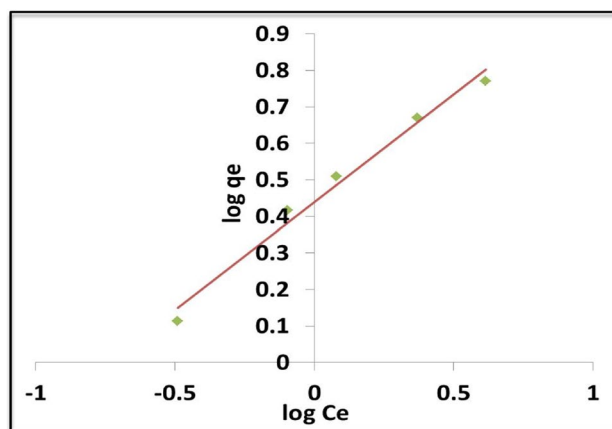
$$\log(q_e - q_t) = \log q_e - \frac{K_1}{2.303} t \tag{7}$$

where  $q_e$  is the amount of dye adsorbed at equilibrium (mg/g),  $q_t$  is the amount of dye adsorbed at any time  $t$  (mg/g), and  $K_1$  is the first-order rate constant ( $\text{min}^{-1}$ ). But the data do not follow pseudo-first-order equation.

#### 3.4.2 Pseudo-second-order

The adsorption equation for pseudo-second-order model is given by following equation:

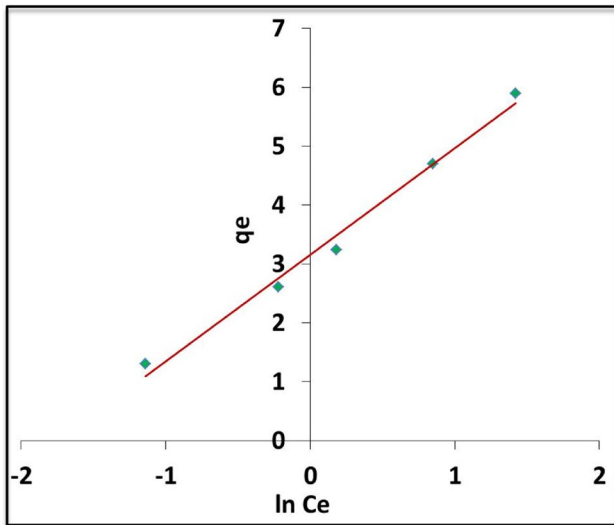
$$\frac{t}{q_t} = \frac{1}{K_2 q_e^2} + \frac{1}{q_e} t \tag{8}$$



**Fig. 8** Freundlich adsorption isotherm for Rh-B adsorption at 305 K

**Table 3** Langmuir, Freundlich, and Temkin isotherms and their constants at different temperatures

Temperature (K)	Langmuir constants				Freundlich constants			Temkin constants		
	$q_m$	$b_L$	$R^2$	$R_L$	$n$	$K_f$	$R^2$	$B$	$K_T$	$R^2$
305	8.52	0.53	0.96	0.045	1.69	2.7	0.97	1.81	5.69	0.98
311	8.76	0.95	0.98	0.031	1.79	2.9	0.98	1.65	7.89	0.98
317	8.90	1.40	0.97	0.010	1.90	3.2	0.97	1.53	9.78	0.97

**Fig. 9** Temkin adsorption isotherm for Rh-B adsorption at 305 K

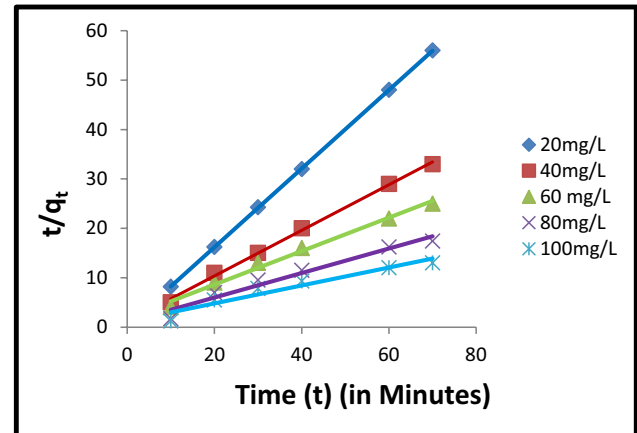
where  $K_2$  is the pseudo-second-order rate constant ( $\text{gmg}^{-1} \text{min}^{-1}$ ),  $q_e$  is the amount of dye adsorbed on the adsorbent at equilibrium ( $\text{mg/g}$ ), and  $q_t$  is the amount of dye adsorbed on the adsorbent at any time  $t$  ( $\text{mg/g}$ ). Figure 10 represents the linear plot of  $t/q_t$  versus  $t$ . It is evident from Fig. 10 that the adsorption process follows the pseudo-second-order kinetics. The value of rate constant  $K_2$  and  $q_e$  have been calculated from plot and are listed in Table 4.

### 3.5 Intra-particle diffusion study

In the batch mode adsorption process, initial adsorption occurs on the surface of the adsorbent and there are chances that adsorbate diffuses into the interior pores of the adsorbent. Weber and Morris suggested the following kinetic model to investigate whether the adsorption is intra-particle diffusion or not. The relationship is given as:

$$q_t = K_{ipd}t^{1/2} + C \quad (9)$$

where  $q_t$  is the amount of dye adsorbed at time  $t$  ( $\text{mg/g}$ ),  $C$  is the constant ( $\text{mg/g}$ ) which gives the thickness of the boundary layer, and  $K_{ipd}$  is the intra-particle diffusion rate constant

**Fig. 10** Pseudo-second-order kinetic model for Rh-B adsorption

( $\text{mg/gmin}$ ). The larger values of  $C$  from the intercept of the plot show that greater is the contribution of surface adsorption. The linear portion in Fig. 11 represents the intra-particle diffusion effect. The correlation coefficients for intra-particle diffusion is very close to unity, thereby indicating that adsorption of Rh-B onto ACTW follows the intra-particle diffusion model. The value of  $K_{ipd}$  and  $C$  are listed in Table 4.

### 3.6 Thermodynamic parameters

The adsorption of Rh-B onto ACTW was studied at three different temperatures, namely 305 K, 311 K, and 317 K, to investigate the feasibility and nature of the process. Thermodynamic parameters such as the free energy change ( $\Delta G$ ), enthalpy change ( $\Delta H$ ), and entropy change ( $\Delta S$ ) were calculated from the variation of the thermodynamic equilibrium constant,  $K_0$ , using equations given below. The values of  $\Delta G$ ,  $\Delta H$ , and  $\Delta S$  for initial concentrations of 20, 40, 60, 80, and 100  $\text{mg/L}$  are presented in Table 5.

$$\Delta G = -RT_1 \ln K_0 \quad (10)$$

$$K_0 = q_e/C_e \quad (11)$$

where  $R$  is the universal gas constant, and  $T$  is the temperature in Kelvin.



**Table 4** Pseudo-second-order kinetic model and intra-particle diffusion values for Rh-B adsorption

$C_0$ (mg/L)	Pseudo-second-order			Intra-particle diffusion parameter		
	$K_2$	$q_e$	$R^2$	$K_{ipd}$	$C$	$R^2$
20	2.46	1.26	0.99	0.006	1.2	0.83
40	0.18	2.17	0.98	0.067	2.1	0.65
60	0.06	3.03	0.99	0.055	2.9	0.75
80	0.055	4.16	1	0.031	4.5	0.95
100	0.027	5.60	1	0.028	5.3	0.97

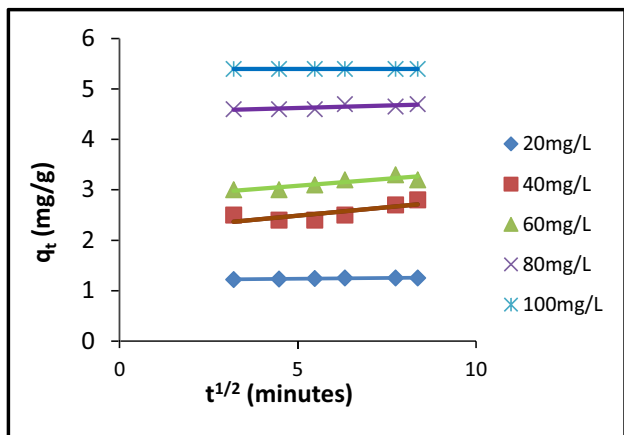


**Fig. 11** Intra-particle diffusion kinetics model for Rh-B adsorption

$$\ln K_0 = \frac{\Delta S}{R} - \frac{\Delta H}{RT} \tag{12}$$

$\Delta H$  and  $\Delta S$  have been calculated from the slope and intercept of the plot between  $\ln K_0$  versus  $1/T$ .

$$\Delta S = \text{Intercept} \times R \tag{13}$$

$$\Delta H = -\text{Slope} \times R \tag{14}$$

where  $R$  is a gas constant ( $8.314 \text{ JK}^{-1}\text{Mole}^{-1}$ ).

Table 5 presents the calculated thermodynamic parameters, including the changes in free energy ( $\Delta G$ ), enthalpy ( $\Delta H$ ), and entropy ( $\Delta S$ ), for the adsorption of Rh-B dye onto ACTW at different initial concentrations (20–100 mg/L) and temperatures (305–317 K). The negative values of  $\Delta G$  indicate

**Table 5** Using pseudo-second-order kinetic model and intra-particle diffusion, the thermodynamically parameters for Rh-B adsorption

$C_0$	$K_0$	$\log K_0$	$\Delta G = -RT \log K_0$			$\Delta H$ (KJ mole <sup>-1</sup> )	$\Delta S$ (KJ mole <sup>-1</sup> K <sup>-1</sup> )
			305 K	311 K	317 K		
20	4.06	1.40	3.55	3.62	3.78	57.49	0.1977
40	3.25	1.17	2.96	3.02	3.18		
60	3.08	1.13	2.86	2.92	2.97		
80	2.00	0.69	1.75	1.79	1.82		
100	1.40	0.336	0.85	0.86	0.88		

that the adsorption process is spontaneous and feasible. The increasing values of  $\Delta G$  with temperature suggest that adsorption becomes more favorable at higher temperatures, possibly due to the enhanced diffusion of dye molecules in solution. The positive values of  $\Delta H$  indicate that the adsorption process is endothermic. The relatively low values of  $\Delta S$  suggest a decrease in entropy at the solid–liquid interface during the adsorption process. Table 6 shows the comparison between the adsorption capacities of different adsorbents derived from various waste products and it was observed that the adsorption capacity of ACTW in the present study was found to be maximum (8.9 mg/g) among these.

### 4 Conclusion

The outcomes of the study demonstrate the potential utility of activated carbon derived from tea waste (ACTW) in effectively eliminating the cationic dye, rhodamine B (Rh-B), from water through adsorption. A thorough investigation

**Table 6** Comparison of adsorption capacity of various adsorbents for rhodamine B removal

Adsorbent	Adsorption capacity (mg/g)	References
Coffee ground powder	5.2	[34]
<i>Mimusops elengi</i> activated carbon	1.7	[35]
Banana peel	3.8	[36]
<i>Chamaecyparis lawsoniana</i> fruit	6.8	[37]
Pomegranate peel	7.3	[38]
Tea waste	8.9	This work

into several key variables, including the initial Rh-B concentration, solution pH, temperature impact, and contact duration, was carried out to optimize the adsorption process. The results revealed that elevating the quantity of ACTW (adsorbent) utilized, ranging from 0.2 g to 1.8 g, led to a corresponding enhancement in Rh-B dye removal efficiency, rising from 76 to 97.8%. Correlations between the isothermal data obtained using the Langmuir, Freundlich, and Temkin equations were meticulously analyzed. FTIR spectra of charcoal and ACTW showed significant difference in the functional groups thereby confirming the activation sites of charcoal. Microimage of ACTW manifests the effect of activation of charcoal with enlarged pores and irregularities in the surface morphology. It can be inferred that ACTW can serve as an economical and efficient adsorbent for the removal of cationic dyes from aqueous solutions, thus highlighting the potential of activated carbon derived from tea waste as a cost-effective solution for the removal of contaminants from water.

**Acknowledgements** The authors are thankful to the Director, Sophisticated Analytical Instrumentation Facility (SAIF) laboratory, Panjab University, Chandigarh, for characterization facility.

**Author contribution** Kanchan Bala: conceptualization, synthesis, and writing.

Deepika Sharma: data curating.

Neeraj Gupta: co-supervision, methodology, and draft writing.

Naveen Kumar: supervision.

Vaseem Raja: reviewing and editing.

**Data availability** Data or material will be made available on reasonable request.

## Declarations

**Ethical approval** The manuscript doesn't involve any testing on human and animal life and doesn't require any ethical approval.

**Conflict of interest** The authors declare no competing interests.

## References

- Wetchakun K, Wetchakun N, Sakulsermsuk S (2019) An overview of solar/visible light-driven heterogeneous photocatalysis for water purification: TiO<sub>2</sub>- and ZnO-based photocatalysts used in suspension photoreactors. *J Ind Eng Chem* 71:19–49
- Bethi B, Sonawane SH, Bhanvase BA, Gumfekar SP (2016) Nanomaterials-based advanced oxidation processes for wastewater treatment a review. *Chem Eng Process Process Intensif* 109:178–189
- Kaur H, Bhatti HS, Singh K (2019) Europium doping effect on 3D flower-like SnO<sub>2</sub> nanostructures: morphological changes, photocatalytic performance and fluorescence detection of heavy metal ion contamination in drinking water. *RSC Adv* 9(64):37450–37466
- Liu H, Liu T, Zhang Z, Dong X, Liu Y, Zhu Z (2015) Simultaneous conversion of organic dye and Cr (VI) by SnO<sub>2</sub>/rGO microcomposites. *J Mol Catal A Chem* 410:41–48
- Zarrin S, Heshmatpour F (2020) Facile preparation of new nano-hybrids for enhancing photocatalytic activity toward removal of organic dyes under visible light irradiation. *J Phys Chem Solids* 140:109271
- Kadirvelu K, Kavipriya M, Karthika C, Radhika M, Vennilamani N, Pattabhi S (2003) Utilization of various agricultural wastes for activated carbon preparation and application for the removal of dyes and metal ions from aqueous solutions. *Biore-sour Technol* 87(1):129–132
- Ito T, Adachi Y, Yamanashi Y, Shimada Y (2016) Long-term natural remediation process in textile dye-polluted river sediment driven by bacterial community changes. *Water Res* 100:458–465
- Imam SS, Babamale HF (2020) A short review on the removal of rhodamine B dye using agricultural waste-based adsorbents. *Asian J Chem Sci* 7(1):25–37
- Jain R, Mathur M, Sikarwar S, Mittal A (2007) Removal of the hazardous dye rhodamine B through photocatalytic and adsorption treatments. *J Environ Manage* 85(4):956–964
- Cuerda-Correa EM, Alexandre-Franco MF, Fernández-González C (2019) Advanced oxidation processes for the removal of antibiotics from water an overview. *Water* 12(1):102
- Droepenu EK, Wee BS, Chin SF, Kok KY, Maligan MF (2022) Zinc oxide nanoparticles synthesis methods and its effect on morphology a review. *Biointerface Res Appl Chem* 12:4261–4292
- Suhan MB, Shuchi SB, Anis A, Haque Z, Islam MS (2020) Comparative degradation study of remazol black B dye using electro-coagulation and electro-Fenton process: kinetics and cost analysis. *Environ Nanotechnol Monit* 14:100335
- Saigl ZM (2021) Various adsorbents for removal of rhodamine b dye: a review. *Indones J Chem* 21(4):1039–1056
- Basheer AA (2018) New generation nano-adsorbents for the removal of emerging contaminants in water. *J Mol Liq* 261:583–593
- Ajiboye TO, Oyewo OA, Onwudiwe DC (2021) Adsorption and photocatalytic removal of rhodamine B from wastewater using carbon-based materials. *Flat Chem* 29:100277
- Moosavi S, Lai CW, Gan S, Zamiri G, Akbarzadeh Pivezhzani O, Johan MR (2020) Application of efficient magnetic particles and activated carbon for dye removal from wastewater. *ACS Omega* 5(33):20684–20697
- Mitra S, Mukherjee T (2018) Novel low cost adsorbent for the removal of rhodamine B dye from wastewater. *IJERM* 05:2349–2058
- Qiu B, Tao X, Wang H, Li W, Ding X, Chu H (2021) Biochar as a low-cost adsorbent for aqueous heavy metal removal: a review. *JAAP* 155:105081
- Mishra D, Jain S, Khare P, Singh R (2023) Comparative investigation of biochar-based nanocomposites over pristine biochar: an overview. *Synthesis, Contaminants Removal, and Environmental Sustainability, Biochar-Based Nanocomposites for Contaminant Management*, pp 57–68
- Moon S, Ryu J, Hwang J, Lee CG (2023) Efficient removal of dyes from aqueous solutions using short-length bimodal mesoporous carbon adsorbents. *Chemosphere* 313:137448
- Lee YJ, Jeong YJ, Cho IS, Park SJ, Lee CG, Alvarez PJ (2023) Facile synthesis of N vacancy g-C<sub>3</sub>N<sub>4</sub> using Mg-induced defect on the amine groups for enhanced photocatalytic OH generation. *J Hazard Mater* 449:131046
- Ahmaruzzaman M, Gayatri SL (2010) Activated tea waste as a potential low-cost adsorbent for the removal of p-nitrophenol from wastewater. *J Chem Eng Data* 55(11):4614–4623
- Olayinka KO, Adu T, Alo BI (2007) Sorption of heavy metals from electroplating effluents by low-cost adsorbents II: use of waste tea, coconut shell and coconut husk.

24. Thapak HK, Trivedia SS, Pandey LK (2015) Tea waste adsorbent for the removal of chromium and copper from synthetic wastewater. *IJRST* 2(2):70–74
25. Chen Z, Shi J, Yang X, Nan B, Liu Y, Wang Z (2015) Chemical and physical characteristics and antioxidant activities of the exopolysaccharide produced by Tibetan kefir grains during milk fermentation. *Int Dairy J* 43:15–21
26. Rao DK, Damodharam T, Yadav JS, Suresh Babu P (2013) Removal of atenolol ( $\beta$ -blocker) from aqueous phase by sorption onto activated charcoal. *Int J Pharm Chem* 2(1):26–32
27. Muthuselvi C, Pandiaraja SS, Ravikumar B, Athimoolam S, Srinivasan N, Krishnakum RV (2018) FT-IR and FT-Raman spectroscopic analyzes of indenoquinoline derivative crystal. *Asian J Appl Sci* 11:83–91
28. Guo Y, Bustin RM (1998) FTIR spectroscopy and reflectance of modern charcoals and fungal decayed woods: implications for studies of inertinite in coals. *Int J Coal Geol* 37(1–2):29–53
29. Allegrini C, Guiliano M, Bourdin M, Mille G (1994) Study of pollutant gas adsorption on activated charcoal using FTIR spectroscopy. *Spectrosc Lett* 27(3):367–377
30. Wong S, Ghafar NA, Ngadi N, Razmi FA, Inuwa IM, Mat R, Amin NA (2020) Effective removal of anionic textile dyes using adsorbent synthesized from coffee waste. *Sci Rep* 10(1):2928
31. Banerjee S, Chattopadhyaya MC (2017) Adsorption characteristics for the removal of a toxic dye, tartrazine from aqueous solutions by a low cost agricultural by-product. *Arab J Chem* 10:S1629–S1638
32. Mensah K, Mahmoud H, Fujii M, Samy M, Shokry H (2022) Dye removal using novel adsorbents synthesized from plastic waste and eggshell: mechanism, isotherms, kinetics, thermodynamics, regeneration, and water matrices. *Biomass Convers Biorefin* 24:1–6
33. Mustapha S, Shuaib DT, Ndamitso MM, Etsuyankpa MB, Sumaila A, Mohammed UM, Nasirudeen MB (2019) Adsorption isotherm, kinetic and thermodynamic studies for the removal of Pb (II), Cd (II), Zn (II) and Cu (II) ions from aqueous solutions using Albizia lebbeck pods. *Appl Water Sci* 9:1–1
34. Shen K, Gondal MA (2017) Removal of hazardous rhodamine dye from water by adsorption onto exhausted coffee ground. *J Saudi Chem Soc* 21:S120–S127
35. Gurunathan V, Gowthami P (2016) The effective removal of rhodamine B dye by activated carbon (MimusopsElengi) by adsorption studies. *Int J Res Inst* 3(21):575–581
36. Singh S, Parveen N, Gupta H (2018) Adsorptive decontamination of rhodamine-B from water using banana peel powder: a biosorbent. *Environ Technol Innov* 12:189–195
37. Gul S, Gul H, Gul M, Khattak R, Rukh G, Khan MS, Aouissi HA (2022) Enhanced adsorption of rhodamine B on biomass of cypress/false cypress (*chamaecyparis lawsoniana*) fruit: Optimization and kinetic study. *Water* 14(19):2987
38. Saigl ZM, Ahmed AM (2021) Separation of rhodamine B dye from aqueous media using natural pomegranate peels. *Indones J Chem* 21(1):212–224

**Publisher's Note** Springer Nature remains neutral with regard to jurisdictional claims in published maps and institutional affiliations.

Springer Nature or its licensor (e.g. a society or other partner) holds exclusive rights to this article under a publishing agreement with the author(s) or other rightsholder(s); author self-archiving of the accepted manuscript version of this article is solely governed by the terms of such publishing agreement and applicable law.